Supplementary Figure Legends

Supplementary Figure 1. Generation of siRNAs for WSX-1 or CNTFR

(A) Expression of WSX-1 in F11 cells. Lysates from F11 cells (50 μg) were subjected to SDS-PAGE and immunoblotted with antibody to the C-terminal region of mouse WSX-1 (mWSX-1-C) (lane 1). Lysates from F11 cells (500 μg) were immunoprecipitated with anti-mWSX-1-C antibody or preimmune serum. The resulting precipitates were subject to SDS-PAGE and immunoblot analysis with the same antibody (lanes 3 and 2). **(B) Efficacy of siRNAs for WSX-1 and CNTFR.** F11 cells were transfected with indicated amounts of the pRNA-U6.1/Shuttle vector (Vec), pRNA-U6.1/Shuttle-mWSX-1 siRNA, or pRNA-U6.1/Shuttle-mCNTFR siRNA. At 72 hr after transfection, cells were harvested for total RNA extraction and immunoblot analysis. Total amounts of transfected vectors were kept constant by the addition of appropriate amounts of the empty vector. Amounts of WSX-1 and CNTFR mRNA expression were determined by real-time PCR and adjusted with those of G3PDH mRNA. Immunoblot analysis was performed with antibodies to mWSX-1-C, CNTFR, and actin. siRNAs for mouse WSX-1 and mouse CNTFR down-regulated mRNA and protein expression of endogenous WSX-1 and CNTFR in F11 cells. F11 cells expressed only mouse-type WSX-1 and CNTFR (data not shown).

Supplementary Figure 2. Knocking down endogenous expression of IL-6R or LIFR does not alter the HN-induced tyrosine phosphorylation of STAT3.

(A) (B) Generation and efficacy of siRNAs for IL-6R and LIFR. siRNAs for mouse IL-6R and LIFR down-regulated mRNA (A) and protein (B) expression of endogenous mouse IL-6R and LIFR in F11 cells. F11 cells were transfected with indicated amounts of the pRNA-U6.1/Shuttle vector (empty), pRNA-U6.1/Shuttle-IL-6R siRNA, or pRNA-U6.1/Shuttle-LIFR siRNA. At 72 hr after transfection, cells were harvested for total RNA extraction and immunoblot analysis. Amounts of IL-6R and LIFR mRNAs were

determined by real-time PCR and adjusted with those of G3PDH mRNA. Immunoblot analysis was performed with antibody to mouse IL-6R, mouse LIFR, and actin. **(C) The siRNA-mediated reduction of endogenous IL-6R or LIFR expression did not attenuate phosphorylation of STAT3 (Tyr^{705}) induced by HNG treatment.** F11 cells were transfected with 0.5 μg of the pRNA-U6.1/Shuttle vector, pRNA-U6.1/Shuttle-IL-6R siRNA, or pRNA-U6.1/Shuttle-LIFR siRNA for 3 hr in the absence of serum. Cells were incubated in HF-18% thereafter. At 24 hr after the onset of transfection, culture media were replaced by Ham's F12 medium containing N2 supplement without FBS. At 72 hr after the onset of transfection, the cells were incubated with 100 ng/ml rat IL-6, 100 ng/ml rat CNTF, or 1 μM HNG at 37°C for 15 min. Cells were harvested for immunoblot analysis with the anti-phosphoSTAT3 (Tyr^{705}) and anti-STAT3 antibodies. Immunoblot analysis with anti-total STAT3 antibody was performed with the same membrane without removal of anti-phosphoTyr^{705} STAT3 antibody just after immunoblot analysis with anti-phosphoTyr^{705} STAT3 antibody was performed. Accordingly, visualized bands in the bottom panel showed both total STAT3- and phosphoTyr^{705} STAT3 -immunoreactivities.

Supplementary Figure 3. HN induced the formation of gp130 and WSX-1 complex in F11 cell. F11 cells (2.5×10^6 cells in10 cm ϕ dish, 2 dishes), incubated with 10 μM HN or 10 μM HNA for 60 min, were harvested for immunoprecipitation with 2 μg of normal rabbit IgG (C) or anti-gp130 (Santa Cruz Biotech, C-20) antibody. Immunoprecipitates were then subject to immunoblot analysis with anti-mouse WSX-1-N antibody or anti-gp130 antibody. One mM BS^3 was added to stabilize the oligomerization during the last 30 min period of co-incubation.

Supplementary Figure 4. Effect of siRNA-mediated knockdown of endogenous Bax on the HN binding to F11 cells.

(A)(B) Generation and efficacy of siRNA for mouse Bax. siRNAs for mouse Bax down-regulated mRNA **(A)** and protein **(B)** expression of endogenous Bax in F11 cells. F11 cells were transfected with 1.0 μg (A) or indicated amounts (B) of the pRNA-U6.1/Shuttle vector (Vector), or pRNA-U6.1/Shuttle-mBax siRNA (si mBax) in the absence of serum for 3 hr. Cells were thereafter incubated in HF-18%. At 72 hr after the onset of transfection, cells were harvested for total RNA extraction and immunoblot analysis. Total amounts of transfected vectors were kept constant by addition of appropriate amounts of the empty vector. Amounts of Bax mRNA expression was determined by real-time PCR and adjusted with those of G3PDH mRNA **(A).** Immunoblot analysis was performed with antibodies to Bax (Santa Cruz Biotech, P-19) and actin (Sigma) **(B). (C) The siRNA-mediated knockdown of endogenous Bax did not reduce the binding of HN to F11 cells.** F11 cells were transfected with 1.0 μg of the pRNA-U6.1/Shuttle vector (vector), 1.0 μg of pRNA-U6.1/Shuttle-mBax siRNA (si mBax), or 0.5 μg of both pRNA-U6.1/Shuttle-WSX-1 siRNA (si mWSX-1) plus 0.5 μg of pRNA-U6.1/Shuttle-CNTFR siRNA (si mCNTFR) for 3 hr in the absence of serum. Cells were thereafter incubated in HF-18%. At 24 hr after transfection, cells were replated onto poly-L-lysine-coated 96-well plates ($7x10^3$ cells/well). At 36 hr after the start of transfection, indicated concentrations of biotin-HN together with or without 100 μM of unlabeled HN or HNA were added. Immunofluorescence-based binding assays were performed, as shown in Materials and Methods.

Supplementary Materials and Methods

SiRNA-encoding plasmids The siRNA vector for mouse FPR2 was described (Hashimoto et al., 2005b). Plasmid vectors encoding small interfering RNAs (siRNAs) for mouse FPR2, CNTFR, WSX-1, IL-6R, LIFR, and Bax were constructed as follows (Sui et al., 2002). The sense and antisense DNA fragments were 5'-AGGATCCCGTAACTACCACTAAGCAATGTCTTGATATCCGGACATTGCTTAGTG GTAGTTATTTTTTCCAAAAGCTTGCA-3' and 5'-TGCAAGCTTTTGGAAAAAATAACTACCACTAAGCAATGTCCGGATATCAAGAC ATTGCTTAGTGGTAGTTACGGGATCCT-3', for mouse FPR2; 5' –TTGGATCCCGTGTGTGCTGTGCCATCCGAGATTGATATCCGTCTCGGATGGCACA GCACACATTTTTTCCAAGGTACCTT-3', 5' –AAGGTACCTTGGAAAAAATGTGTGCTGTGCCATCCGAGACGGATATCAATCTCG GATGGCACAGCACACACGGGATCCAA-3' for mouse CNTFR; 5'-TTGGATCCCATATCCACTTGAGAGAAGATCTTGATATCCGGATCTTCTCTCAAG TGGATATTTTTTTCCAAGGTACCTT-3', 5'-AAGGTACCTTGGAAAAAAATATCCACTTGAGAGAAGATCCGGATATCAAGATC TTCTCTCAAGTGGATATGGGATCCAA-3' for mouse WSX-1; 5'-GCGGATCCCGTTTAAGCTGTGAAACGCTTCGTTGATATCCGCGAAGCGTTTCA CAGCTTAAATTTTTTCCAAAAGCTTGC-3', and 5'-GCAAGCTTTTGGAAAAAATTTAAGCTGTGAAACGCTTCGCGGATATCAACGAA GCGTTTCACAGCTTAAACGGGATCCGC-3' for mouse IL-6R; 5'-GCGGATCCCGTCAATCCTGTGAAATACTGCCTTGATATCCGGGCAGTATTTCAC AGGATTGATTTTTTCCAAAAGCTTGC-3', and 5'-GCAAGCTTTTGGAAAAAATCAATCCTGTGAAATACTGCCCGGATATCAAGGCAGT

ATTTCACAGGATTGACGGGATCCGC-3'for mouse LIFR; 5'-CGGGATCCCATGATCTGTTCAGAGCTGGTGTTGATATCCGCACCAGCTCTGAACAGATCATTTTTTTCCAAGGTACCCC-3' and 5'-GGGGTACCTTGGAAAAAAATGATCTGTTCAGAGCTGGTGCGGATATCAACACCAGCTCTGAACAGATCATGGGATCCCG-3' for mouse Bax. These DNA fragments were annealed by heating and cooling according to the manufacturer's instructions.

Real-time PCR Real-time PCR analysis was performed using a QuantiTect SYBR Green PCR kit (QIAGEN), followed by analysis with ABI PRISM7700 (Applied Biosystems, Foster City, CA) (Kanekura et al., 2005). Data analysis was performed using software Sequence Detection System ver. 1.9.1 (Applied Biosystems). To adjust the expression levels of each mRNA, the levels of G3PDH mRNA were used as internal controls. We made sets of a sense primer and an antisense primer as follows; (5'- TTCCACCGTGACTCCTG CACCTG-3', 5'-GAGGGCTGGGTCCTTCTCACA GAC-3') for mouse CNTFR; (5'-CCGCAGAAAGCTCTCACCTGTCAG-3, 5'-CCATGGATATCCGTTCTCCACCTG-3') or for mouse WSX-1; (5'-GTGGAAGATACGTCGGCAGACTCG-3', 5'-ACCCTGAAGGTCAGCAATCCTCAG-3') for mouse LIFR; (5'-CCCTGCCAGTATTCTCAGCAGCTG-3', 5'-CGGCCTTCCAGGTATGGCTGATAC-3') for mouse IL-6R; (5'-GGAATTCACCATGGACGGGTCCGGGGAGCAG-3', 5'-GGGGTACCGCCCATCTTCTTCCAGATGGTGAG-3') for mouse Bax; and (5'-TCCACCACCCTGTTGCTGTA–3' and 5'-ACCACAGTCCATGCCATCAC–3') for human and mouse G3PDH.

Supplementary Figure 1

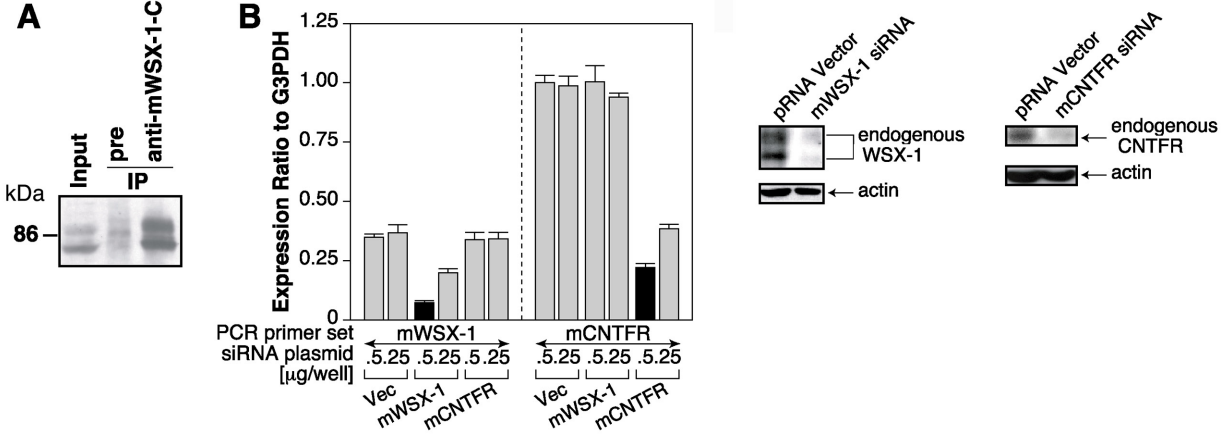

Supplementary Figure 2

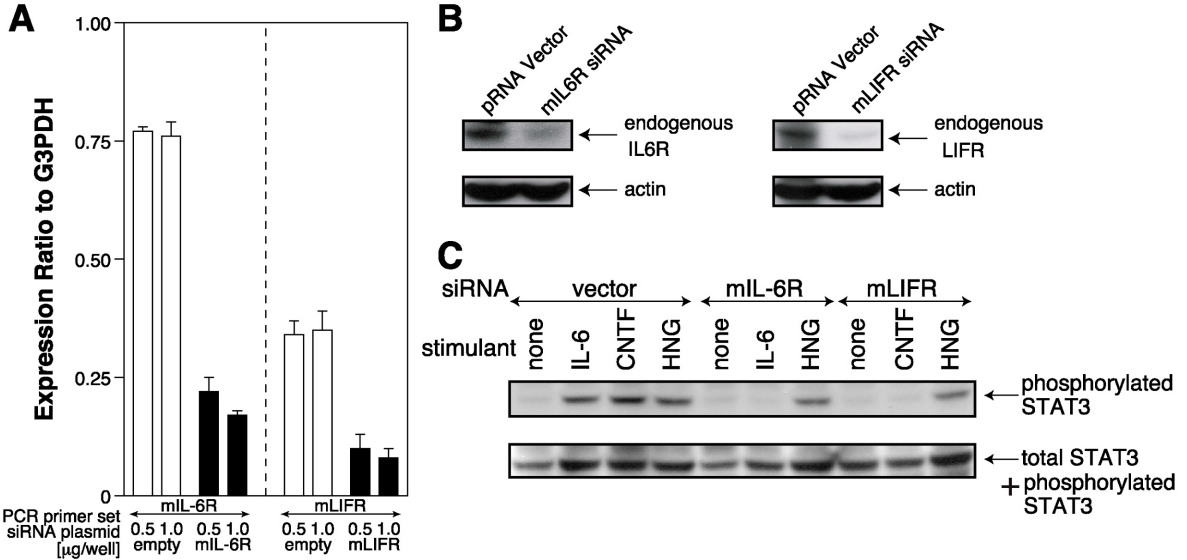

Supplementary Figure 3

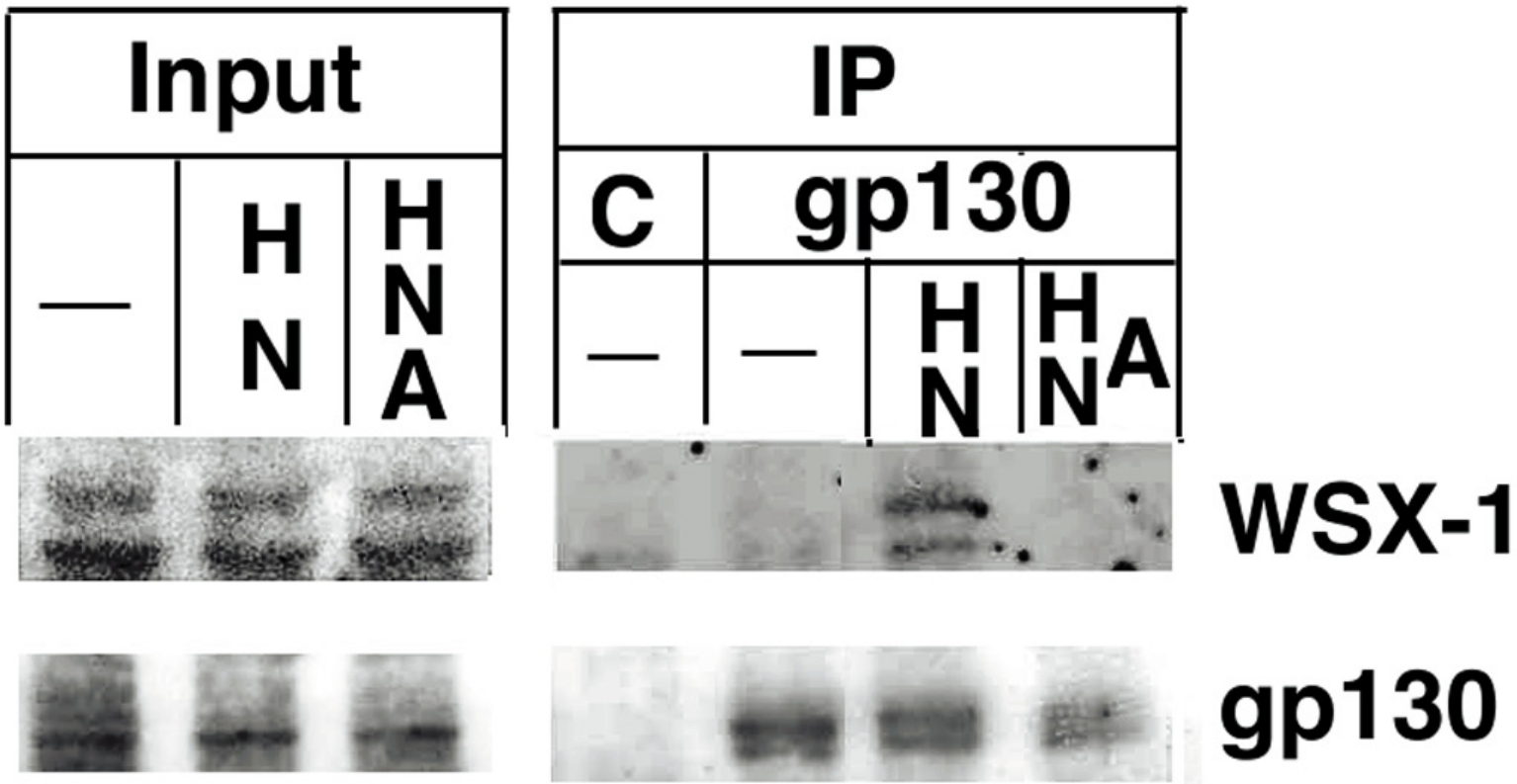

Supplementary Figure 4